Original Article

Development And Toxicological Evolution Of Pegylated Chitosan Nanoparticle For The Simultaneous Delivery Of Silymarin And Dehydroemetine For The Enhance Hepatic Targeting

Saurabh Arjariya[1*], Ritesh Jain[2], Neeraj Sharma[3]

[1*]Faculty of pharmacy, Madhyanchal professional University, Bhopal (462044), Madhya Pradesh, India.
[2,3]Professor, Madhyanchal professional University, Bhopal (462044), Madhya Pradesh, India.

Corresponding Author:* Saurabh Arjariya

*****Research Scholar (PhD*), Faculty of Pharmacy, Madhyanchal professional University, Bhopal (462044), Madhya Pradesh, India. Email Address:-arjariya.saurabh@gmail.com, Cont. No: - +91-9425141117
DOI:10.47750/pnr.2022.13.S08.617

Abstract

The objective of the current study was to create biodegradable pegylated chitosan nanoparticles (SDNPs) and assess their potential for hepatic targeting on a single platform. The hepatoprotective effect of silymarin (SM) and dehydroemetine (DH) to the liver was investigated using the PEGylated chitosan nanoconjugate. Ionic gelation process was used to create the PEGylated Chitosan Nanoparticles, which were then tested for several optical and in-vitro characteristics. The MTT experiment on a human hepatocyte cell line revealed IC50 values for SDNPs and SM-DH of 0.45 and 0.67 M, respectively. The assessment of in vitro cell lines confirms improved uptake and biodistribution findings from confocal microscopy and apoptosis assay, which notably demonstrated increased accumulation of nanoconjugates in brain compared to free API. Compared to prohibited medications, the targeting of prospective SDNPs was found to be two times as significant. This leads to the conclusion that bidoegradable PEgylated chitosan nanoconjugates can be employed as possible nano-targeting to attach PEGylated chitosan nanoparticles for improved delivery of hepatoprotective medicines to the liver for better therapeutic outcome.

Keywords: PEgylation; Nanoparticles; Silymarin-Dehydroemetine; Hepatoprotective; Liver targeting

1. INTRODUCTION

One of the most common organs in the human body is the liver. The liver's primary duties include bile secretion, detoxification, fat, protein, and carbohydrate metabolism. The primary site (Liver) for intense metabolism and excretion has little to offer in terms of modern medicine (1). Any physiochemical, biochemical, and morphological alterations to the liver's normal function are referred to as hepatic disorders. Any alteration in liver function that results in illness is known as liver disease. Many vital bodily processes are carried out by the liver, and if it develops a disease or is harmed, those processes may cease, which could cause serious harm to the body. Hepatic disease is another name for liver disease [2- 3].

The phrase "liver disease" is a general one that refers to any possible issues that could arise and prevent the liver from carrying out its intended duties. Before a decline in function happens, often more than 75%, or three quarters, of the liver tissue must be compromised. Therefore, herbal medications play a major role in treating hepatic disorders and have an unexpected impact on maintenance and performance [4-5]. Chitosan is the second most prevalent biopolymer after cellulose and is a naturally occurring polysaccharide produced when chitin is alkaline deacetylated.

Chitosan has been widely used in the food industry for applications such as metal chelation in wastewater, water purification, clarification and deacidification of fruit juice, formation of edible films, and preservation of foods against microbial deterioration due to its good properties of non-toxicity, good biocompatibility, mechanical film forming ability, and antimicrobial activity [6]. Recent research has demonstrated the potential of using chitosan in the food industry for regulated delivery systems of active agents in the form of micro- or nanospheres. Chitosan microspheres typically need to be cross-linked in order to extend the time and controlled release property of active agents. Many chemical crosslinkers, including glutaraldehyde, formaldehyde, glyoxal, and other reactive cross-linking agents, have been employed [7].

The ancient medicinal plant Silybum marianum L. (Milk Thistle), a member of the Carduus marianum family, has been used for millennia to cure a variety of illnesses, including liver and gallbladder issues, protecting the liver from snakebites and bug stings, mushroom poisoning, and alcoholism [8]. The very first usage of Milk thistle, however, was for its hepatoprotectant and antioxidant activities. The major flavonoids in this herb, silymarin, include silybin A, silybin B, isosilybin A, and isosilybin B, as well as other flavonoids including silychristin, neosilyhermin, silyhermin, and silydianin, which are more prevalent in the fruit and seeds than the other portions [9-10].

A synthetic antiprotozoal drug called dehydroemetine is comparable to emetine in structure and anti-amoebic characteristics (the main difference being a double bond next to the ethyl group), but it has less adverse effects [11-12]. Roche produces it for the American market. The Centres for Disease Control once dispensed it on a compassionate use basis as an experimental medicine to treat metronidazole-resistant amoebiasis, but they no longer do so [13].

In the current study, we combined natural and synthetic chemicals to form the two medicines Silymarin and Dehydroemetine and encapsulated them in biodegradable chitosan nanoparticles [14]. The PEGylated Nurtured Chitosan Nanoparticles were used as a stable and protective carrier for hepatic targeting against hepatoprotective potential, incorporating natural Silymarin with synthetic dehyroemetine [15]. In this study, we have shown that PEGylated CS nanoparticles have increased targeted potency, allowing us to combine two drugs to treat hepatic disorders with significant liver targeting and potentially synergistic effects [16].

2. MATERIALS AND METHODS:

The API Silymarin (SM) and dehydroemetine (DH) was obtained as gift sample from Taj Pharmaceuticals Ltd, Hyderabad, India. Chitosan with medium molecular weight (M.W. =750 000 Da) was purchased from Himedia (India). PEG (poly ethylene glycol was purchased from Sigma Aldrich, Bengaluru, India. Dialysis membrane (Mol. wt. cut-off: 12 000 Dalton, flat with 25 mm, diameter of 16 mm) was purchased from Himedia (India). High purity water was used for all experiments, prepared by using (Millipore). All other chemicals and reagents were of analytical grade.

2.1 Preparation of PEgylated Chitosan Nanoparticles

For the formulation of chitosan nanoparticles, acuurately weighed Silymarin and dehydroemetine were individually encapsulated using the ionotropic gelation process. In a 1% v/v aqueous glacial acetic acid (GAA) solution, 100 mg of accurately weighed both SM and DH were along with 0.4% w/v Chitosan were dissolved. At a rate of 2 ml/min, 0.4% Sodium Tripolyphosphate Solution (TPP) was added drop by drop to the drug polymer solution (12 ml TPP to 20 ml drug polymer solution) [17]. To create nano-sized particles, the resultant particle dispersion was sonicated for five minutes at a medium amplitude (50%) using a probe sonicator (S-4000; Misonix, Farmingdale, NY). In order to ensure maximum transportation at the intended site, the dispersion was then filtered through a 0.2 um hydrophilic filter (Minsart, Sartorius) for the isolation of smaller nanosize particles. The resulting nano-sized particles were thoroughly filtered using ultrafiltration against double-distilled water at the ideal temperature (Amicon 8200 with a millipore PBMK membrane, MWCO 300000). The ultrafiltration makes it easier to get rid of unbound drugs and solvent residue. For the PEgylation procedure, precisely 50 mL of 0.3% chitosan nanoparticles were added to a 3:1 solution of polyethylene glycol (PEG), which was then agitated for one hour at 500 rpm. In addition, dispersion was used for 60 seconds on the mixture to create uniform PEG-Chitosan nanoparticles [18].

3. CHARACTERIZATION

3.1 Particle size, Zeta potential and pH analysis

Malvern Zetasizer 3000, a particle size and zeta potential analyser, was used to measure the developed SDNPs particle size, and surface charge (Malvern Instruments, Bedfordshire, UK). By smearing the electrophoretic mobility of particles in an applied electrical field, the Zeta potential of developed SDNPs was investigated [19]. The nano formulation concentrations were set at 0.01% w/v by distilled water or in a 0.01 M sodium chloride solution for prospective evaluation. Through the use of a digital pH metre, the pH was determined (HI-TECH WATER TECH. New Delhi, India). The pH metre was initially calibrated using a buffer tablet, and after calibration the pH metre was submerged in a beaker containing sample of SDNPs nanoformulations [20]. An average value with SD was provided after the nanoformulations' evaluation and measurement were performed three times each.

3.2 Dynamic light scattering analysis

Using the Brook-heaven BI 9000 AT equipment, the SDNPs nanoformulation was evaluated for the Dynamic Light Scattering (DLS) investigation of mean diameter and PDI (Brookheaven Instrument Corporation, USA). The more distinct and substantial evaluation of SDNPs nanoformulations was measured using the DLS examination. SDNPs nanoformulation was evaluated using DLS at wavelengths of 287 nm, respectively, at a temperature of 25 °C [21].

3.3 TEM (Transmission Electron Microscopy) Analysis

Using a Hitachi H-7500 TEM analyzer, the TEM of SDNPs nanoformulation was measured. To visualise the shape and structure of the nanoformulation, TEM pictures were obtained. The SDNPs was put in a copper disc grid and covered with a 2.5% w/v solution of phosphor-tungstic acid (PTA). The grid was then placed in the disc holder and dried using a 60-watt LED lamp (Philips, India Ltd.). This was followed by a TEM evaluation scan.

3.4 SEM (Scanning Electron Microscopy) Analysis

By using a SEM, the Nova Nano SEM 450, Germany, the morphology and structure of the produced SDNPs nanoformulation was examined. The formulations were lyophilized using a freeze-dry lyophilizer prior to the SEM analysis (REMI, New Delhi, India). Dual adhesive tape was then used to attach the dry formulations to a SEM stub at 50 mA for 5 to 10 minutes using a sputter (KYKY SBC-12, Beijing, China) [23]. To obtain digital photos of the created SDNPs nanoformulation, a SEM with a secondary electron detector was used.

3.5 Entrapment Efficiency (EE) analysis

In order to achieve the predicted therapeutic benefit, EE is crucial in delivering the bioactive to the targeted region at the precise therapeutic dose. The SDNPs nanoformulation were spun at 10,000 rpm for 5 minutes to generate pellets for the EE measurement. The drug concentration was measured spectrophotometrically using a UV spectrophotometer (Schimadzu, Japan) at 287 nm for the SDNPs nanoformulation, against a blank solvent after the collected supernatant was carefully diluted with PBS of pH 7 [24]. The following formula can be used to calculate the EE:

EE= weight of drug in nanoformulation / initial weight of drug taken x 100

3.6 In-vitro drug release analysis

It was possible to predict the diffusion and kinetic behaviour of the nanosystem for the intended therapeutic efficacy by monitoring the release of from SDNPs nanoformulation. The SDNPs produced from centrifugation were suspended in 10 mL of a phosphate buffered saline (PBS) solution with a pH of 7.4 for release tests [25]. This suspension of nanoparticles was transferred to a clean Eppendorf's tube and heated to 37 °C while being stirred. Samples were taken out of the bath after 0.5, 1, 2, 4, 6, and 24 hours and centrifuged for 5 minutes at 14 000 rpm (BOECO, Hamburg, Germany). The amount of medication released from the nanoparticles over the allotted time was calculated from supernatants using UV spectroscopic analysis [26]. An average value with SD was provided after the nanoformulations' evaluation and measurement were performed three times each.

3.7 Cell Line studies

3.7.1 Cell culture and seeding

The NCCs in Pune provided the Primary Human hepatocytes cells line (PHH-C), which was preserved in Dulbecco's modified Eagles Medium. The cell line was then given 10% foetal bovine serum (FBS), 100 U/mL penicillin, and 100 g/mL streptomycin antibiotic solution from PAA Laboratories GmbH in Austria. The Primary Human hepatocytes cells line (PHH-C) was cultivated in tissue culture flasks (75 cm2) and conserved at 5% CO2 atmosphere at 37°C. After getting the 90% confluency, the cells were trypsinized with 0.25% trypsin EDTA solution (Sigma, USA) (Sigma, USA). The Primary Human hepatocytes cells line (PHH-C) were seeded in 6 well plates (Costars, Corning Inc., NY, USA) at a density of 50,000 cells per well for additional statistical qualitative cell uptake and apoptosis analysis [27].

3.7.2 Cell uptake assay by CLSM

Confocal laser microscopy (CLSM) was used to conduct a qualitative cell uptake assay in order to evaluate the dispersal potential of a nanoformulation utilising Primary Human hepatocytes cells line (PHH-C). For 3 hours, the cells were gestated with SDNPs formulation, and free drug Silymarin and dehydroemetin (SM-DH) (each at a concentration of 1 g/ml). Following the gestation period, the media around the formulations were washed three times with Hanks buffered salt solution (PAA Laboratories GmbH, Austria) and examined by CLSM (Olympus FV1000) [28].

3.7.3 MTT assay

For the MTT assay, the Primary Human hepatocytes cells line (PHH-C) was seeded in 96-well plates and incubated with media containing SDNPs, and free SM-DH (equivalent concentration of 0.1, 1, 10, and 20 g/mL), as well as a negative control (cells treated with normal saline solution) and a positive control (Tri cells were washed three times with HBSS after the media containing the samples had been incubated for 24 hours. The MTT solution (500 g/mL in PBS) was then added to each well and incubated once more for 4 hours. The formazan crystals were subsequently dissolved in 200 L of DMSO after the MTT solution had been articulated after 4 hours. After the 4h articulated MTT solution, the formazan crystals were subsequently dissolved in 200 L of DMSO.

3.7.4 Apoptosis assay

The free drug Silymarin and dehdroemetin (SM-DH) , as well as their ability to cause apoptosis Primary Human hepatocytes cells line (PHH-C), were all tested for their ability to induce cell cytotoxicity. The Phosphatidylserine disclosure on the plasma membrane's outer layer and its interaction with Annexin V provide the foundation for the Annexin V apoptosis assay [31]. In a nutshell, 6 well cell culture plates were seeded with Primary Human hepatocytes cells line (PHH-C), and they were then cultured overnight at 37°C and 5% CO2. The media was then articulated, replaced with media containing free SM-DH (equal to 10 g/mL), and SDNPs formulation for a total of 6 hours of gestation. Following incubation, the medium was removed, the cells were treated with Annexin V Cy3.18 (AnnCy3) and 6-carboxyfluorescein di-acetate (6-CDFA) using the Annexin V Cy3 TM Apoptosis Detection kit from Sigma. USA. The Primary Human hepatocytes cells line (PHH-C) was then seen using CLSM with 6-CDFA and AnnCy3 in the red and green channels, respectively [32]. It was also possible to measure the apoptosis index, which is the fluorescence strength ratio between the red channel, which measures apoptosis, and the green channel, which measures vitality. Using Image J software, the fluorescence signals in the photographs were estimated (U.S. National Institutes of Health, Bethesda, Maryland, USA). By dividing the percentage of apoptotic cells (annexin+) by the overall percentage of cells in the sample (apoptotic [annexin+] plus no apoptotic cells [annexin-]), one can get the apoptotic index (AI). The apoptotic index was determined using the following formula:

AI=%AV+C/ (%AV+C+%AV-C)

Where %AV+C represent the percentage of annexin V positive cell and %AV-C represent the percentage of annexin V negative cells [33].

3.8 Statistical Analysis

Mean ± SD was used to express the values. Statistics. One-way analysis of variance (ANOVA) was used to statistically analyse the data, and a result of $p>0.01$ ($n = 3$) was deemed significant [34].

4 RESULTS & DISCUSSION

The incorporation of the pawn anion TPP into the steady Chitosan polymer solutions resulted in the impulsive synthesis of PEGylated chitosan nanoparticles encasing the SM-DH. Ionic interactions between the negatively charged ion TPP and the positively charged amino groups of chitosan led to the production of nanoparticles. To achieve stable dispersion and the creation of nanosize particles, the ratio of CS/TPP was tuned. To determine the ideal concentrations of CS and TPP for NPs production, preliminary experiments were carried out. To produce physiochemically and thermally stable nanoparticles, both the process and formulation parameters were carefully tuned. A transparent solution, an opalescent suspension with a tyndall effect (NPs), or other types of widely described nano-sized particles were the three main categories of the obtained particles.

4.1 Particle size, Zeta potential & pH analysis

The synthesised SDNPs formulations were measured using a zeta sizer, and the findings showed significantly distinct sizes ranging from 120 to 190 nm **(Figure 1 c).** Due to formulation and process improvement, the SDNPs formulation showed nano size respectable encapsulation of API in the polymer matrix. The surface charges of the two nanoformulation, SDNPs were established to be -11.019 mV, respectively **(Figure 1 e**), indicating that the formulations are negative in charge. The formulation's negative charge demonstrated improved stability and the best qualification for improved liver targeting. The pH of SDNPs formulation was found to be 6.3 ± 1.98, which is critical for effective liver targeting and virtually neutral microenvironment delivery. The primary factor in the onsite breakdown of the polymer matrix is the pH facilitate targeting mechanism. By enhancing the drug release at a controlled rate, this polymeric degradation activation mechanism produced the required therapeutic potential.

4.2 Dynamic Light scattering analysis

The synthesised SDNPs nanoformulation exhibits nanosize range dispersion according to the DLS once again. The size distribution patterns of the nanoformulation are rather similar to the claimed one, with the size ranges for SDNPs formulations being 120–150 nm. The ideal range of nanosizes for SDNPs showed improved liver transport and onsite targeting that effectively complied with cell size and its microenvironment. Diverse size distribution and dispersion patterns were revealed by the DLS research. The PDIs of SDNPs was found to be 0.301± 0.02. The produced nanoparticles' enhanced stability and even size distribution pattern were shown by the DLS results to range between 100 and 300 nm **(Figure 1 d).** This stable nanoscale shape makes it easier for prepared nanoparticles to diffuse through hepatic membrane barriers, which results in the best possible pharmacological potential during liver targeting. Consequently, it can be categorically said that the nanoformulation demonstrated ideal and stable nano dispersion properties for the active liver targeting against hepatoprotective treatment in clinical platform.

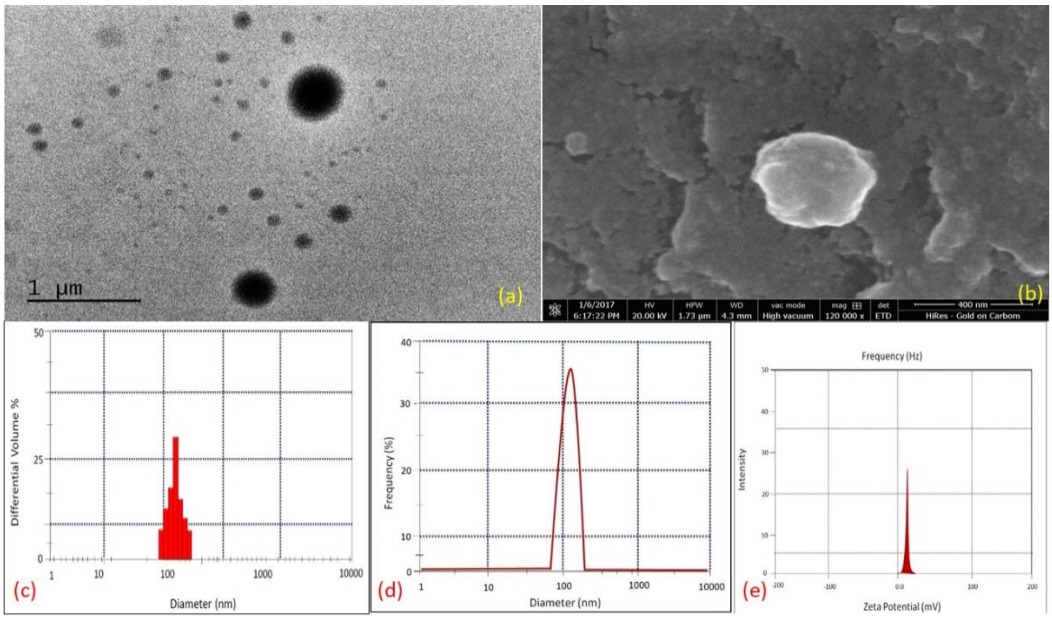

Figure 1: Image a & b illustrating TEM and SEM investigation of developed SDNPs at nano scale resolution respectively, whereas image c elaborating size distribution pattern by zeta sizer measurement, image d & e showing the DLS pattern and zeta potential of developed SDNPs respectively, (mean ± SD, n=3)

4.3 TEM analysis

The TEM investigation revealed very small, oval-shaped nanoparticles of both nanoformulations that were quite distinct in size. The DLS measuring zeta sizer analysis was validated by the size range disclosed by TEM analysis for SDNPs,

which was 100–200 nm **(Figure 1a)**. By encasing natural extracts, nanoparticles were created that had improved crosslinking between the cross linker and the polymer, preventing undesired leakage. Additionally, it was discovered that nanoparticle aggregation was minimal, demonstrating improved PEGylation of chitosan boundaries The TEM results showed an appropriate nano carrier system for the efficient transport to the liver, displaying respectable hepatic membrane penetration appearance of the developed nanoformulation.

4.4 SEM Analysis

Zeta sizer and TEM assay results revealing the generation of small particles with spherical shape and smooth morphology were greatly improved by SEM analysis. The sharp oval margins of the nanoformulation, which showed a better PEGylation process, are noteworthy validated by the SEM pictures. The SEM pictures also make clear that no evidence of cluster formation or particle aggregation with a discernible PEG outer layer is present. The excellent brain targeted delivery features of SDNPs were confirmed by the zeta-sizer analysis and the SEM analysis, both of which showed size ranges of 100-180 nm **(Figure 1b)**.

4.5 In-vitro drug release profile

The Figure 3 shows the in vitro drug release data of Silymarin and dehydroemtin combination loaded in PEGylated nanoformulations. At different pH (5.0 & 7.4), the drug release pattern from the SDNPs displayed a non-linear release profile characterised by a considerably rapid initial drug release over the first 3–4 h, followed by a slower release in the latter period **(Figure 2 a & b)**. The two pH range was offered to thoroughly assess the impact of nanoformulation for better on-site distribution and liver targeting. The SDNPs showed the biphasic drug release pattern, with the initial bursting of nanoparticles in the early 1–8 h and the gradual release in the following 24 h. According to in-vitro drug release tests, at pH 4.0, SDNPs initially provided a burst release of the drug extract. For nanoformulation sample, the drug release was discovered to be 86.15 ± 1.08% at 6h, 89.13 ± 0.45%, at 8h, 91.16 ± 2.63% at 16h, and 94.08 ± 2.74 % at 24h, respectively. On the other hand, at pH 7, the SDNPs showed uneven type of drug release of about 80% which was found insignificant (P >0.05) delayed compared to pH 4.

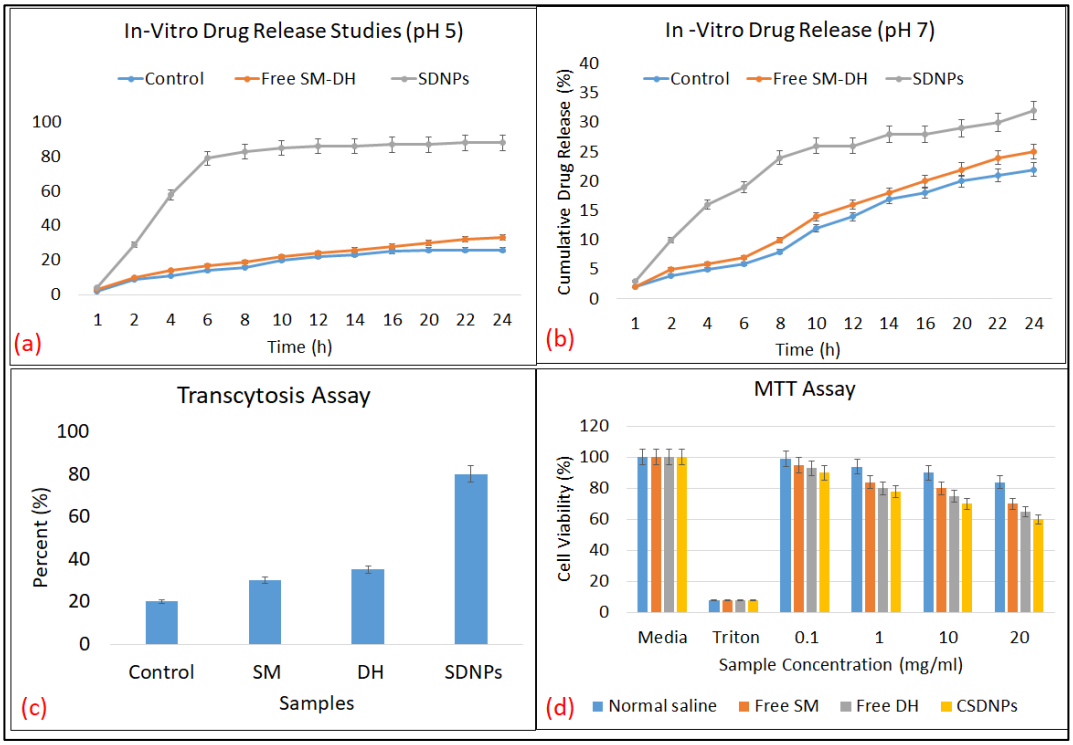

Figure 2: Image a and b elaborating the combination drug release kinetics of developed SDNPs at pH 4 and 7 using dialysis bag membrane, whereas image c & d showing Transcytosis assay and MTT cell toxicity measurement of developed SDNPs on primary human hepatocytes cells line (PHH-C) on 24 hr of incubation, (mean ± SD, n=3)

4.7 Cell line studies

The Primary Human hepatocytes cells line (PHH-C) was used to assess and measure the produced nanoformulation SDNPs for cellular targeting and intracellular transport. The PHH-C cell line is a crucial component of the hepatic membrane system and is widely used to examine hepatic delivery. When examined by CLSM analysis, the produced SDNPs demonstrated notable cellular uptake and circulation in comparison to the free Silymarin and Dehydroemetin. When treated with Rhodamine B isothiocyanate (RITC), the CLSM signals for the generated SDNPs were more robust and crisp with improved absorbance when compared to the free drug SM-DH combination solution after incubation for 12 h. **(Figure 3).** Additionally, the nanoformulations' bright fluorescence signals captured by confocal laser scanning microscopy clearly indicated the location of nanoparticles within vesicles, suggesting enhanced endocytic pathway advancement. When compared to the cells treated with SDNPs incubated at 4 h and 12 h of time periods, the CLSM

signals shown by free drug samples treated Primary Human hepatocytes cells line (PHH-C) revealed meagre red fluorescence signal surrounding the cell nucleus, which is shown to be enhanced and significant. According to the results of the CLSM intensity examination, The SDNPs had two times greater in vitro cellular uptake and resilience on the membranes of brain cells than free SM-DH combination. Inductively coupled plasma optical emission (ICP-OE) spectrometry was used to quantitatively observe the SDNPs treated cells during the course of a 12-hour incubation period. The transwell assay at the basolateral side of the experiment successfully proves that around 50% of SDNPs and 30% of free drug solution nanoformulation have specifically crossed into the hepatic membrane layer. The free drug extracts demonstrated insufficient intracellular transport and penetration efficiency through primary human hepatocytes cells line (PHH-C) of just 16%, indicating early cell membrane adsorption limited direct diffusion to the cells (Figure 3c). Overall, at various incubation times, SDNPs for cell uptake and transportation was exceptional compared to free drug solution (SM-DH) with potent fluorescent advertisements devoid of any morphological variation in cell lines, leading to improved brain targeting effectiveness.

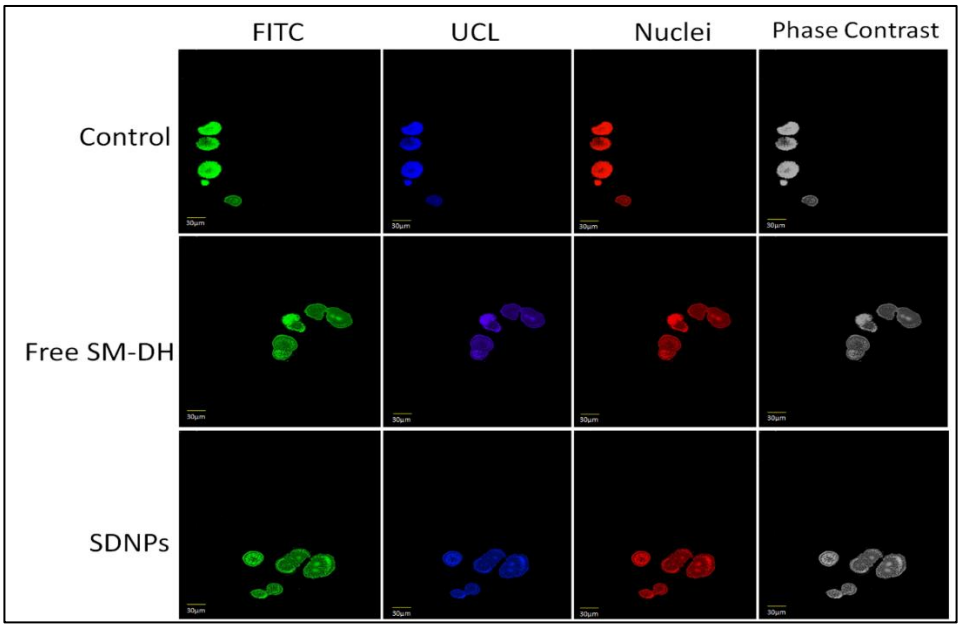

Figure 3: illustration of in-vitro cellular uptake and CLSM localization measurement on primary human hepatocytes cell line by developed free drug Silymarin and dehydroemetine combination and developed SDNPs equated with normal control normal saline treated cell at 30µm scale bar after 12 h incubation respectively, *p<0.05 and *p<0.01 compared to the untreated cell, (mean + SD, n=3),

4.8 MTT assay

For the investigation of developed SDNPs against primary human hepatocytes cells line (PHH-C), the MTT test was used. After 24 hours of incubation, the MTT assay qualitatively demonstrated the nanoformulation considerable anti-proliferation efficacy. The investigations revealed that the Triton X 100 surfactant solution negative control group and the normal control group both had sharp cell viability of 100% and 10%, respectively. Following a 24-hour incubation period, the produced SDNPs demonstrated noteworthy cell viability of 95%, 85%, 71%, and 66% respectively **(Figure 2 c and d).** While free drug solution demonstrated cell viability of 90%, 75%, 61%, and 41%, respectively, after 24 hours of incubation. A nonlinear relationship between incubation time and anti-proliferation effectiveness was demonstrated by the MTT research, which found non-significant cell cytotoxicity by several substances after 24 hours of incubation. The MTT results clearly showed that, after 24 hours of incubation, the nanoformulation was significantly more cell-viable than the free drug extract, demonstrating biologically safe brain targeting effectiveness with barely detectable toxicity on human hepatocytes cells. The improved physiochemical compatibility of the SDNPs which results in effective cellular transport and liver delivery, is the cause of the enhanced cell viability. When comparing free drug solution combination had lower cell viability than SDNPs at higher concentrations. When assessed by a student's T test, the inter-comparison results revealed improved endocytosis and robustness of SDNPs, which is proven to be statistically significant. The created nanocomposite may be employed as a unique drug carrier encasing natural extract for the treatment of liver illnesses as a targeted delivery system, according to the results of the cell toxicity tests.

4.9 Apoptosis Assay

The Apoptosis experiment demonstrated remarkable apoptosis at all concentrations using free drug solution and developed SDNPs. In contrast to the free drug combination, the SDNPs exhibited intrinsic apoptosis. The developed SDNPs were found to exhibit the cell surface receptor-induced mitochondrial apoptosis phenomenon or death activator. The intended apoptosis process is achieved by activating the caspase cascade, which is accomplished by activating the cell surface receptor. The Silymarin and dehydroemetin combination solution showed the apoptosis indices of 0.39 compared to the SDNPs apoptotic indices of 0.78, respectively. In comparison to free drug combination solution and

normal saline solution (apoptotic index 0.20), The SDNPs showed two folds strong apoptotic effect (*P> 0.01). **(Figure 4).** The nanosized particles, which result in speedy onsite drug transportation, adequate distribution, and superior release, are the main reason why nanoformulation exhibits better apoptosis than free drug solution. When assessed using a student T test, the apoptotic potential between SDNPs and free drug solution is significantly higher compared to normal saline control group. Overall, PEgylation of chitosan nanoparticles promotes improved nanoparticle circulation in the hepatic microenvironment, resulting in prolonged release and low drug toxicity, leading to superior hepatic targeting against heptoprotective efficiency.

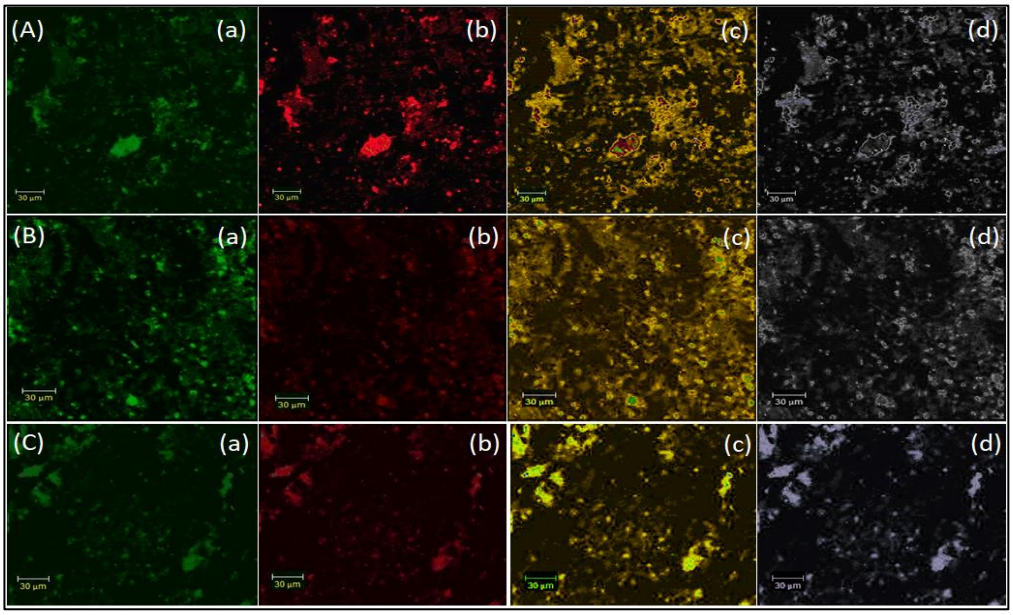

Figure 4: Images A, B, S and D elaborating the apoptosis measurment of free drug Silymarin and dehydroemetine combination with developed SDNPs (10 µg/ml; 6h incubation) on primary human hepatocytes cell line (PHH-C); (a) green channel representing the fluorescent signal from carboxy fluorescein (cell viability marker dye); (b) overlay images of figure, (c) red channels showing fluorescein signals from Annexin Cy 3.18 (cell apoptosis marker dye); (d) depicting differential contrast images of cells. The fluorescence intensities of the images were measured using Image J software, U. S. National Institutes of Health, Bethesda, Maryland, USA, http://imagej.nih.gov/ij/. (n=3, data expressed as average ± SE,*denotes p<0.01).

5 SUMMARY AND CONCLUSION

For improved liver delivery and targeting, combination of Silymarin and dehydroemetin have been successfully entrapped and studied in PEGylated chitosan-based nanoparticles in the current investigations. The initial finding confirmed a stable optimization process with variable drug and polymer system size and encapsulation capacity to regulate extract release. With the aid of various physiochemical techniques, including TEM and SEM, as well as other qualitative assessments, the produced nanoformulation system was carefully described. This validated the creation of spherical-shaped nanoparticles free of any unintended agglomeration. For improved liver targeting, the in-vitro drug release mechanism demonstrated sustained drug release from nano vesicles, and the cytotoxicity examination revealed notable cell viability of the nanoformulation at all concentrations. The in-vitro cyto-compatibility tests confirm the enhanced cell trans-cytosis signals with enhanced cell uptake and dispersion of SDNPs by cell proliferation CLSM evaluations. The novel hepatic targeting via natural extract encapsulated biodegradable nano vesicle system, however, is supported by recent advancements in nanomedicine and offers better and more effective nano-therapy to target the liver than conventional formulations with advantages of low dose frequency, increased bioavailability, and good patient compliance.

6. CONFLICT OF INTEREST

The authors declare no conflict of interest

7. REFERENCES

1. Elsawy H., Badr G.M., Sedky A., Abdallah B.M., Alzahrani A.M., Abdel-Moneim A.M. Rutin ameliorates carbon tetrachloride (CCl_4)-induced hepatorenal toxicity and hypogonadism in male rats. *PeerJ.* 2019;7:e7011. doi: 10.7717/peerj.7011. [PMC free article] [PubMed] [CrossRef] [Google Scholar]
2. Chen Q., Zhang H., Cao Y., Li Y., Sun S., Zhang J., Zhang G. Schisandrin B attenuates CCl4-induced liver fibrosis in rats by regulation of Nrf2-ARE and TGF-β/Smad signaling pathways. *Drug Des. Dev. Ther.* 2017;11:2179. doi: 10.2147/DDDT.S137507. [PMC free article] [PubMed] [CrossRef] [Google Scholar]
3. Köhler U.A., Böhm F., Rolfs F., Egger M., Hornemann T., Pasparakis M., Weber A., Werner S. NF-κB/RelA and Nrf2 cooperate to maintain hepatocyte integrity and to prevent development of hepatocellular adenoma. *J. Hepatol.* 2016;64:94–102. doi: 10.1016/j.jhep.2015.08.033. [PubMed] [CrossRef] [Google Scholar]
4. Shimozono R., Asaoka Y., Yoshizawa Y., Aoki T., Noda H., Yamada M., Kaino M., Mochizuki H. Nrf2 activators attenuate the progression of nonalcoholic steatohepatitis–related fibrosis in a dietary rat model. *Mol. Pharmacol.* 2013;84:62–70. doi: 10.1124/mol.112.084269. [PubMed] [CrossRef] [Google Scholar]

5. Niu L., Cui X., Qi Y., Xie D., Wu Q., Chen X., Ge J., Liu Z. Involvement of TGF-β1/Smad3 signaling in carbon tetrachloride-induced acute liver injury in mice. *PLoS ONE.* 2016;11:e0156090. doi: 10.1371/journal.pone.0156090. [PMC free article] [PubMed] [CrossRef] [Google Scholar]
6. Supriono S., Nugraheni A., Kalim H., Eko M.H. The Effect of Curcumin on Regression of Liver Fibrosis through Decreased Expression of Transforming Growth Factor-β1 (TGF-β1) *Indones. Biomed. J.* 2019;11:52–58. doi: 10.18585/inabj.v11i1.463. [CrossRef] [Google Scholar]
7. Mohseni R., Karimi J., Tavilani H., Khodadadi I., Hashemnia M. Carvacrol ameliorates the progression of liver fibrosis through targeting of Hippo and TGF-β signaling pathways in carbon tetrachloride (CCl_4)-induced liver fibrosis in rats. *Immunopharmacol. Immunotoxicol.* 2019;41:163–171. doi: 10.1080/08923973.2019.1566926. [PubMed] [CrossRef] [Google Scholar]
8. Zhang Y., Liu J., Ma Y., Wang J., Zhu J., Liu J., Zhang J. Integration of high-throughput data of microRNA and mRNA expression profiles reveals novel insights into the mechanism of liver fibrosis. *Mol. Med. Rep.* 2019;19:115–124. doi: 10.3892/mmr.2018.9641. [PMC free article] [PubMed] [CrossRef] [Google Scholar]
9. Gjorgjieva M., Sobolewski C., Ay A.-S., Abegg D., Correia de Sousa M., Portius D., Berthou F., Fournier M., Maeder C., Rantakari P. Genetic ablation of MiR-22 fosters diet-induced obesity and NAFLD development. *J. Pers. Med.* 2020;10:170. doi: 10.3390/jpm10040170. [PMC free article] [PubMed] [CrossRef] [Google Scholar]
10. Roulot D., Sevcsik A.M., Coste T., Strosberg A.D., Marullo S. Role of transforming growth factor β type II receptor in hepatic fibrosis: Studies of human chronic hepatitis C and experimental fibrosis in rats. *Hepatology.* 1999;29:1730–1738. doi: 10.1002/hep.510290622. [PubMed] [CrossRef] [Google Scholar]
11. Hong Y., Cao H., Wang Q., Ye J., Sui L., Feng J., Cai X., Song H., Zhang X., Chen X. MiR-22 may suppress fibrogenesis by targeting TGFβR I in cardiac fibroblasts. *Cell. Physiol. Biochem.* 2016;40:1345–1353. doi: 10.1159/000453187. [PubMed] [CrossRef] [Google Scholar]
12. Fukushima T., Hamada Y., Yamada H., Horii I. Changes of micro-RNA expression in rat liver treated by acetaminophen or carbon tetrachloride−regulating role of micro-rna for RNA expression. *J. Toxicol. Sci.* 2007;32:401–409. doi: 10.2131/jts.32.401. [PubMed] [CrossRef] [Google Scholar]
13. Robinson T.F., Cohen-Gould L., Factor S.M., Eghbali M., Blumenfeld O.O. Structure and function of connective tissue in cardiac muscle: Collagen types I and III in endomysial struts and pericellular fibers. *Scanning Microsc.* 1988;2:1005–1015. [PubMed] [Google Scholar]
14. Hafez M.M., Hamed S.S., El-Khadragy M.F., Hassan Z.K., Al Rejaie S.S., Sayed-Ahmed M.M., Al-Harbi N.O., Al-Hosaini K.A., Al-Harbi M.M., Alhoshani A.R., et al. Effect of ginseng extract on the TGF-β1 signaling pathway in CCl_4-induced liver fibrosis in rats. *BMC Complement. Altern. Med.* 2017;17:45. doi: 10.1186/s12906-016-1507-0. [PMC free article] [PubMed] [CrossRef] [Google Scholar]
15. Liu L., Wang Q., Wang Q., Zhao X., Zhao P., Geng T., Gong D. Role of miR29c in goose fatty liver is mediated by its target genes that are involved in energy homeostasis and cell growth. *BMC Vet. Res.* 2018;14:325. doi: 10.1186/s12917-018-1653-3. [PMC free article] [PubMed] [CrossRef] [Google Scholar]
16. Bansal M.B., Chamroonkul N. Antifibrotics in liver disease: Are we getting closer to clinical use? *Hepatol. Int.* 2019;13:25–39. doi: 10.1007/s12072-018-9897-3. [PubMed] [CrossRef] [Google Scholar]
17. Ebrahimi H., Naderian M., Sohrabpour A.A. New concepts on reversibility and targeting of liver fibrosis; A review article. *Middle East J. Dig. Dis.* 2018;10:133. doi: 10.15171/mejdd.2018.103. [PMC free article] [PubMed] [CrossRef] [Google Scholar]
18. Gillessen A., Schmidt H.H.-J. Silymarin as supportive treatment in liver diseases: A narrative review. *Adv. Ther.* 2020;37:1279–1301. doi: 10.1007/s12325-020-01251-y. [PMC free article] [PubMed] [CrossRef] [Google Scholar]
19. De Avelar C.R., Pereira E.M., De Farias Costa P.R., De Jesus R.P., De Oliveira L.P. Effect of silymarin on biochemical indicators in patients with liver disease: Systematic review with meta-analysis. *World J. Gastroenterol.* 2017;23:5004. doi: 10.3748/wjg.v23.i27.5004. [PMC free article] [PubMed] [CrossRef] [Google Scholar]
20. Abenavoli L., Aviello G., Capasso R., Milic N., Capasso F. Milk thistle for treatment of nonalcoholic fatty liver disease. *Hepat. Mon.* 2011;11:173–177. [Google Scholar]
21. Pérez-Sánchez A., Cuyàs E., Ruiz-Torres V., Agulló-Chazarra L., Verdura S., González-Álvarez I., Bermejo M., Joven J., Micol V., Bosch-Barrera J., et al. Intestinal permeability study of clinically relevant formulations of silibinin in Caco-2 cell monolayers. *Int. J. Mol. Sci.* 2019;20:1606. doi: 10.3390/ijms20071606. [PMC free article] [PubMed] [CrossRef] [Google Scholar]
22. Saller R., Meier R., Brignoli R. The use of silymarin in the treatment of liver diseases. *Drugs.* 2001;61:2035–2063. doi: 10.2165/00003495-200161140-00003. [PubMed] [CrossRef] [Google Scholar]
23. Gu X., Manautou J.E. Molecular mechanisms underlying chemical liver injury. *Expert Rev. Mol. Med.* 2012;14:e4. doi: 10.1017/S1462399411002110. [PMC free article] [PubMed] [CrossRef] [Google Scholar]
24. Bonferoni M.C., Gavini E., Rassu G., Maestri M., Giunchedi P. Chitosan Nanoparticles for Therapy and Theranostics of Hepatocellular Carcinoma (HCC) and Liver-Targeting. *Nanomaterials.* 2020;10:870. doi: 10.3390/nano10050870. [PMC free article] [PubMed] [CrossRef] [Google Scholar]
25. Jeon T.I., Hwang S.G., Park N.G., Jung Y.R., Im Shin S., Choi S.D., Park D.K. Antioxidative effect of chitosan on chronic carbon tetrachloride induced hepatic injury in rats. *Toxicology.* 2003;187:67–73. doi: 10.1016/S0300-483X(03)00003-9. [PubMed] [CrossRef] [Google Scholar]
26. Teksoy O., Sahinturk V., Cengiz M., İnal B., Ayhancı A. The Protective Effects of Silymarin on Thioacetamide-Induced Liver Damage: Measurement of miR-122, miR-192, and miR-194 Levels. *Appl. Biochem. Biotechnol.* 2019;191:528–539. doi: 10.1007/s12010-019-03177-w. [PubMed] [CrossRef] [Google Scholar]
27. Kim M., Yang S.-G., Kim J.M., Lee J.-W., Kim Y.S., Lee J.I. Silymarin suppresses hepatic stellate cell activation in a dietary rat model of non-alcoholic steatohepatitis: Analysis of isolated hepatic stellate cells. *Int. J. Mol. Med.* 2012;30:473–479. doi: 10.3892/ijmm.2012.1029. [PMC free article] [PubMed] [CrossRef] [Google Scholar]
28. Meng S., Yang F., Wang Y., Qin Y., Xian H., Che H., Wang L. Silymarin ameliorates diabetic cardiomyopathy via inhibiting TGF-β1/Smad signaling. *Cell Biol. Int.* 2019;43:65–72. doi: 10.1002/cbin.11079. [PubMed] [CrossRef] [Google Scholar]
29. Chen Q., Lu H., Yang H. Chitosan inhibits fibroblasts growth in Achilles tendon via TGF-β1/Smad3 pathway by miR-29b. *Int. J. Clin. Exp. Pathol.* 2014;7:8462. [PMC free article] [PubMed] [Google Scholar]
30. Potdar P.D., Shetti A.U. Evaluation of anti-metastatic effect of chitosan nanoparticles on esophageal cancer-associated fibroblasts. *J. Cancer Metastasis Treat.* 2016;2:259–267. doi: 10.20517/2394-4722.2016.25. [CrossRef] [Google Scholar]
31. Sooklert K., Nilyai S., Rojanathanes R., Jindatip D., Sae-Liang N., Kitkumthorn N., Mutirangura A., Sereemaspun A. N-Acetylcysteine reverses the decrease of DNA methylation status caused by engineered gold, silicon, and chitosan nanoparticles. *Int. J. Nanomed.* 2019;14:4573. doi: 10.2147/IJN.S204372. [PMC free article] [PubMed] [CrossRef] [Google Scholar]
32. Calvo P., Remuñán-López C., Vila-Jato J.L., Alonso M.J. Novel hydrophilic chitosan-polyethylene oxide nanoparticles as protein carriers. *J. Appl. Polym. Sci.* 1997;63:125–132. doi: 10.1002/(SICI)1097-4628(19970103)63:1<125::AID-APP13>3.0.CO;2-4. [CrossRef] [Google Scholar]
33. Mitra A., Dey B. Chitosan microspheres in novel drug delivery systems. *Indian J. Pharm. Sci.* 2011;73:355. [PMC free article] [PubMed] [Google Scholar]
34. Sipoli C.C., Santana N., Shimojo A.A.M., Azzoni A., de la Torre L.G. Scalable production of highly concentrated chitosan/TPP nanoparticles in different pHs and evaluation of the in vitro transfection efficiency. *Biochem. Eng. J.* 2015;94:65–73. doi: 10.1016/j.bej.2014.11.008. [CrossRef] [Google Scholar]